

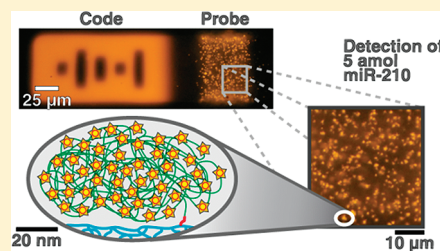
Ultrasensitive Multiplexed MicroRNA Quantification on Encoded Gel Microparticles Using Rolling Circle Amplification

Stephen C. Chapin and Patrick S. Doyle*

Department of Chemical Engineering, Massachusetts Institute of Technology, Cambridge, Massachusetts 02139, United States

Supporting Information

ABSTRACT: There is great demand for flexible biomolecule analysis platforms that can precisely quantify very low levels of multiple targets directly in complex biological samples. Herein we demonstrate multiplexed quantification of microRNAs (miRNAs) on encoded hydrogel microparticles with subfemtomolar sensitivity and single-molecule reporting resolution. Rolling circle amplification (RCA) of a universal adapter sequence that is ligated to all miRNA targets captured on gel-embedded probes provides the ability to label each target with multiple fluorescent reporters and eliminates the possibility of amplification bias. The high degree of sensitivity achieved by the RCA scheme and the resistance to fouling afforded by the use of gel particles are leveraged to directly detect miRNA in small quantities of unprocessed human serum samples without the need for RNA extraction or target-amplification steps. This versatility has powerful implications for the development of rapid, noninvasive diagnostic assays.



The growth of molecular diagnostics requires innovative tools that are sensitive, specific, and precise enough to quantify low levels of multiple biological targets simultaneously in complex media in a single assay. To minimize assay development time and cost, these systems should be flexible enough to allow for rapid probe-set modification, standard postassay analysis methods, and the interrogation of diverse classes of clinically relevant biomolecules. MicroRNAs (miRNAs) are small noncoding RNAs that have been shown to have powerful predictive value in determining diagnosis and prognosis for several diseases including cancer, diabetes, and Alzheimer's.^{1–4} It has proven difficult, however, to accurately and efficiently quantify this increasingly important target set in biological samples due to high levels of sequence homology, complex secondary structures, and wide ranges of natural abundance.⁵ Microarray, deep sequencing, and PCR-based approaches for miRNA quantification provide high sensitivity but ultimately are ill-suited for the high-throughput analysis of small, focused clinical target panels, an application space that is quickly expanding due to interest in personalized medicine.^{6–9} With shorter, customizable workflows and rapid postassay analysis options, particle-based arrays offer a more economical solution for such applications, but the relatively poor sensitivity of commercially available particles requires significantly larger sample amounts.^{10–13} The ideal platform for the analysis of focused miRNA biomarker panels would provide high sensitivity and specificity, scalable multiplexing with a simple workflow, and the ability to directly interrogate easily obtainable biological samples without the need for RNA extraction.

It has recently been shown that miRNAs are remarkably stable in the RNase-rich environment of blood because of their association with the Argonaute2 ribonucleoprotein complex and membrane-bound vesicles.^{14,15} As a result, these small noncoding RNAs

have become an attractive target set for the development of noninvasive blood-based bioassays and for the study of novel mechanisms of intercellular communication.^{15–18} Unfortunately, the quantification of circulating miRNAs is particularly challenging due to low levels of natural abundance as well as the biological complexity of blood and its derivatives (plasma and serum). While microarray and PCR-based methods have been developed to profile serum-based miRNAs, all existing approaches require RNA isolation and/or target amplification, which complicates assay workflow as well as quantification.^{16–18} The development of efficient diagnostic assays in this biological medium requires a highly sensitive multiplexing platform capable of direct target detection in minute amounts of sample without the need for complex, time-consuming processing and purification steps.

In order to enhance the sensitivity of a biological assay, one can either amplify the number of targets present in a sample or amplify the reporting signal produced by each of the targets. Target-based amplification via PCR has been widely used as a means to profile low-abundance miRNA.⁹ However, great care must be taken in the optimization of primer sequences to prevent amplification bias in multiplexed assays and to ensure accurate quantification of target amounts. Signal-based amplification improves sensitivity without augmenting the number of target molecules and, as a result, offers a more direct route to biomolecule quantification, even allowing for single-molecule reporting resolution. Several signal amplification strategies have been adapted for the quantification of miRNA, including rolling circle amplification (RCA) and isothermal ramification

Received: June 24, 2011

Accepted: August 3, 2011

Published: August 03, 2011

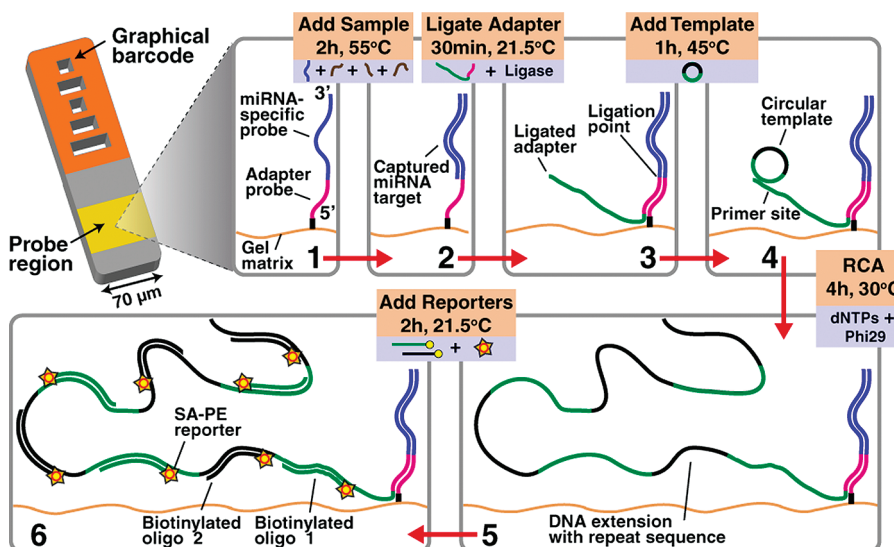


Figure 1. Gel particle RCA workflow. A graphical barcode consisting of unpolymerized holes in the wafer structure of the particle indicates the miRNA-specific probe embedded within a different region of the gel. Particles are incubated with sample, after which a universal adapter sequence with a primer site is ligated to the 3' end of all captured targets and a circular template is allowed to anneal. Phi29 polymerase and dNTPs are incubated in a custom reaction buffer at 30 °C to generate a DNA extension with repeat sequences, each of which can be labeled with two distinct biotinylated oligonucleotides attached to streptavidin-phycoerythrin (SA-PE).

amplification (RAM).^{10,19–22} In these approaches, the polymerase-mediated replication of a circular template is used to create long DNA concatemers either in solution or immobilized on a substrate that can be labeled with multiple fluorophores or radioactive isotopes, thereby amplifying the signal generated from a single target molecule to a level that can be observed using standard detection instruments. Although significant enhancements in detection performance have been achieved with signal-based amplification, the limits of detection (LODs) demonstrated with such approaches remain considerably higher than those obtained with quantitative PCR,¹⁰ preventing their use in emerging applications such as the direct quantification of multiple miRNAs from single cells or easily obtainable body fluids.

We sought to investigate the use of RCA for multiplexed miRNA quantification on graphically encoded hydrogel micro-particles that have previously exhibited high-performance detection properties.^{11,23} Created with the use of the microfluidic process of stop-flow lithography (SFL),^{24,25} these gel particles bear spatially segregated chemical regions for encoding and target capture. A series of unpolymerized holes in the wafer structure of the fluorescently doped “code” region indicates the identity of the DNA probe or probes covalently immobilized on and within separate “probe” regions of the gel particle. In a typical assay, a custom mix of particles bearing DNA probes complementary to the desired target miRNA sequences are exposed to a sample solution, specific targets are captured on the immobilized probes, and the captured miRNA molecules are then fluorescently labeled for quantification. The selective labeling of only those miRNAs that have been specifically captured on immobilized probes has several advantages over the bulk enzymatic and chemical methods used in the majority of direct detection schemes, including higher efficiency, lower cost, and reduced likelihood of labeling bias due to secondary structure.^{6,26,27} In previous work with these particles, we demonstrated a post-target-hybridization labeling procedure that ligated a universal

adapter sequence with a single fluorophore to each target captured on or within the microgel particles for attomole-level miRNA quantification and rapid dysregulation analysis in low-input human total RNA for cancer profiling.¹¹ Because the same adapter can be used for *all targets* in a multiplex assay, this scheme provides a convenient means for developing signal-based amplification without the risk of sequence bias.

In this paper, we describe the use of RCA to achieve subfemtomolar multiplexed quantification of miRNA on encoded microgels with single-molecule reporting resolution. We incorporate a primer site into the 3' end of the universal adapter, and then we extend each ligated adapter (Figure 1) through the introduction of a circularized DNA template and Phi29 DNA polymerase, a highly processive enzyme capable of more than 50 000 base insertions per binding event.²⁸ The enzyme's excellent strand displacement allows for the use of small circular templates, the repeated “rolling” of which results in the production of extensions bearing hundreds of replicate sequences that can each be fluorescently labeled through the hybridization of appropriately decorated reporter oligonucleotides (Figure 1). This method greatly expands the utility of our multifunctional gel particle platform^{11,23,25,29} by enhancing sensitivity to a level that allows for the direct detection of miRNA in small amounts of serum without the need for RNA extraction or potentially biasing target-amplification steps. With RCA and fluorescent spot-based quantification, we achieve miRNA detection sensitivity superior to that of existing particle arrays, RCA approaches, and conventional microarrays.¹⁰

EXPERIMENTAL SECTION

Particle Synthesis. Particles were simultaneously synthesized, encoded, and functionalized with rhodamine and DNA probe in 38 μm tall polydimethylsiloxane (PDMS, Sylgard 184, Dow Corning) microfluidic channels with SFL at a rate of 16 000 particles/h.^{11,24} Code regions and inert spacers (i.e., regions with

no rhodamine or probe) were polymerized from monomer solutions with 35% (v/v) poly(ethylene glycol) diacrylate (MW 700 g/mol) (PEG-DA 700, Sigma Aldrich), 20% poly(ethylene glycol) (MW 200 g/mol) (PEG 200, Sigma Aldrich), 40% 3× Tris-EDTA (TE, USB Corporation) buffer (pH 8.0), and 5% Darocur 1173 photoinitiator (Sigma Aldrich). Code prepolymer was formed by combining code monomer with 1× TE and rhodamine-acrylate (1 mg/mL, Polysciences) to give final concentrations of 9.4% and 0.6%, respectively. Inert prepolymer was formed by combining inert monomer with 1× TE and blue food coloring to give final concentrations of 8.0% and 2.0%, respectively. Probe regions on single-probe particles were polymerized from a monomer solution that was added to acrydite-modified DNA probe sequences (Integrated DNA Technologies, IDT) suspended in 1× TE to give 60 μM probe in 18% PEG-DA 700, 36% PEG 200, 35% 3× TE, 6.5% 1× TE, and 4.5% Darocur. The probe concentration was chosen to match the conditions used for miR-210 and miR-221 detections in a previous study.¹¹ It should be noted that particle capture efficiency and thus sensitivity could be increased by raising the probe concentration (up to 400 μM has been used). For multi-probe particles, the miR-210 probe prepolymer was modified to allow for stream visualization during synthesis; a portion of the 3×TE was replaced with blue food coloring (final concentration of 2%).

As described elsewhere,¹¹ prepolymer solutions were injected into microfluidic synthesis channels, coflowing laminar streams were exposed to brief UV bursts through transparency masks, and the resulting hydrogel particles were collected in TET (1× TE with 0.05% Tween-20 surfactant (Sigma Aldrich)), rinsed, and stored at final concentrations of ~12.5 particles/μL in a refrigerator (4 °C) for later use. Tween-20 was required to prevent particle aggregation. For single-probe particles, stream widths were adjusted during synthesis procedures to create code and probe regions that spanned 140 and 45 μm, respectively, of the length of the particles. Inert regions accounted for the remaining 65 μm of the length.

RCA Assay Protocol. All assays were conducted in 0.65 mL Eppendorf tubes using a total reaction volume of 50 μL and a final NaCl concentration of 350 mM. Previous miRNA multiplexing experiments with gel particles and ligation-based labeling determined 350 mM NaCl to be optimal for achieving highly specific target binding with short incubation times.¹¹ For all preliminary experiments and calibration trials, a hybridization buffer (TET with NaCl), ~20 particles of each type, and appropriately diluted synthetic RNA target sequences (IDT; sequence IDs from miRBase release 17) were added (in that order) to the reaction tube. Depending on assay type, either 0.5 μL of TET or 0.5 μL of *E. coli* total RNA (200 ng/μL) was also added. Circular template for RCA was prepared using CircLigase (Epicentre Biotechnologies) and the protocol described in Schopf et al.³⁰ Following circularization, template was stored at -20 °C for future use. The primer sequence and template used in this study were based on the system described in Schopf et al.,³⁰ with an alteration made to the primer site to reduce hairpin melting temperature and optimize performance (see the Supporting Information).

Target incubation was conducted at 55 °C for 2 h in a thermomixer (Multi-Therm, Biomega; used for all incubation steps at 1500 rpm setting). After target capture, particles were washed three times with a rinse solution of 500 μL of TET with 50 mM NaCl ("R50"), using centrifugation at 6000 rpm (Galaxy MiniStar, VWR) to pull particles to the bottom of the tube for

manual aspiration and exchange of carrier solution. For all rinses in this study, 50 μL of solution was left at the bottom of the tube to ensure retention of particles. A primer-modified universal adapter sequence was then ligated to all captured targets at 21.5 °C for 30 min using T4 DNA ligase (New England Biolabs) and New England Buffer no. 2 (NEB2, New England Biolabs).¹¹

Following adapter ligation, particles were washed three times in R50 and circular template was added to give a final concentration of 50 nM. Template was allowed to anneal to the primer site during a 1 h incubation at 45 °C, after which particles were washed two times in R50. Prior to the addition of the RCA reagents, particles were also washed with 235 μL of a gel-customized RCA buffer consisting of 10% 10× NEB2 and 90% TET solution. Bovine serum albumin (BSA, New England Biolabs), dithiothreitol (DTT, Epicentre), dNTPs (Epicentre), and Phi29 polymerase (Epicentre) were then added to give final concentrations of 200 μg/mL, 5 mM, 150 μM (of each dNTP), and 400 U/mL, respectively. RCA was performed at 30 °C for the desired extension time, followed by three washes in R50. Two biotinylated reporter sequences were added to give a final concentration of 50 nM each and incubated with the particles for 1 h at 21.5 °C. Particles were washed three times in R50 and incubated with 2.5 μL of a 1:50 dilution of SA-PE (1 mg/mL) for 1 h at 21.5 °C. Finally, particles were washed three times in R50 and one time in PTET (5× TE with 25% PEG 400 and 0.05% Tween-20). For analysis, 13 μL of particle solution was placed on a cover glass (24 mm × 60 mm, VWR), sandwiched with another smaller cover glass (18 mm × 18 mm, VWR), and imaged using a CCD camera (Andor Clara) attached to an inverted microscope (Zeiss Axio Observer) equipped with a 20× objective (Zeiss Plan-Neofluar, 0.5 NA), UV source (Lumen 200, Prior), and filter set (XF101-2, Omega).

Serum Assay. Sera taken from one healthy donor and from one donor with prostate cancer were obtained from BioServe Biotechnologies (donors were matched by age, sex, and race). Aliquots (25 μL) were prepared immediately upon receipt and kept frozen at -20 °C until assay. For all assays, 22.5 μL of a modified TET incubation buffer was added to the serum to denature background proteins as well as RNA-induced silencing complex (RISC)-associated proteins known to sequester miRNAs.¹⁵ Assuming standard physiologic NaCl concentration of 150 mM in human serum,³¹ the TET incubation buffer was supplemented with appropriate amounts of NaCl, SDS, and Tween-20 to give concentrations of 350 mM, 2% (w/v), and 0.05% (v/v), respectively, in the final 50 μL reaction volume. Following addition of the buffer, each sample was heated to 90 °C for 10 min and then allowed to cool for 2 min. Next, SUPERase-In RNase inhibitor (Applied Biosystems) was added to each sample to give a concentration of 0.5 U/μL in the final 50 μL reaction volume. Particles and synthetic RNA target were then added, and the samples were placed in a thermomixer at 55 °C for 2 h. The remainder of the assay was identical to the procedure described above. During optimization of the serum assay, the 90 °C preheating step was found to be essential for eliminating nonspecific adsorption of material during target incubation, presumably due to its effective disruption and denaturation of background proteins.

RESULTS AND DISCUSSION

RCA Optimization. Although RCA has been widely used to enhance signal transduction on solid surfaces,^{30,32–34} there is

limited information on the technique's performance on gel-based substrates.^{35,36} Our hydrogel particle platform is highly advantageous for bioassays, as it has proven to be both bioinert and nonfouling in complex biological media.²⁹ However, careful optimization must be undertaken when introducing new labeling reagents that can alter the environment of the stimuli-responsive microgels. To evaluate the compatibility of RCA and our microgels, we created particles with a probe region embedded with a previously described DNA sequence capable of capturing miR-210 target and our universal adapter sequence.¹¹ Upon testing the detection of 10 amol of synthetic miR-210 RNA with a primer-modified adapter and two commercial RCA buffers from New England Biolabs (Ipswich, MA) and Epicentre Biotechnologies (Madison, WI), we observed significant nonspecific binding of fluorescent labels on all portions of the particles. In an attempt to isolate the reagent(s) responsible, we prepared several "knockout" buffers using NEB2, which had proven to be compatible with the gel particles during earlier ligation studies. Each knockout buffer either eliminated one of the constituents of the commercial RCA buffers altogether or reduced it to the lower level found in NEB2. When the Tris-HCl concentration was reduced from 40–50 mM to 10 mM in the RCA buffer, the majority of the fouling was eliminated without negatively impacting the amplification process, indicating that lower buffer pH was responsible for the nonspecific adsorption onto the gel matrix. The remaining noise was removed by supplementing the customized buffer with BSA at a concentration of 200 $\mu\text{g}/\text{mL}$. In separate experiments, incubation conditions and the concentrations of circular template, DTT, dNTPs, Phi29 polymerase, and reporter sequences were adjusted to ensure the highest possible signal-to-noise ratio (see the Supporting Information).

For the low target amounts considered in this study (<50 amol), the vast majority of the target-binding events occurred on probes immobilized near the surface of the hydrogel particle. This can be attributed to the probe-target reaction rate being relatively fast compared to target diffusion through the gel matrix, as well as the fact that the collection of probes near the surface will avoid saturation.^{11,23,25} Because of this binding pattern, we imaged the top and bottom faces of each tablet-shaped particle in order to quantify the fluorescent signal arising from target-binding. For higher target amounts, fluorescence was integrated over the top and bottom faces of each probe region and then averaged. For lower amounts where individual DNA-reporter coils could be distinguished, fluorescent spots on the top and bottom faces of each probe region were summed.

We investigated the effect of RCA extension time on signal intensity by incubating 5 amol of synthetic miR-210 with ~ 20 particles bearing an appropriate probe (Figure 2). The number of discernible spots increased over the first 4 h of extension, but there was no noticeable difference in spot count between RCA times of 4 and 8 h. However, the fluorescence intensity of each spot increased throughout the examined time range, with evidence of a plateau emerging by hour 16. The higher signal intensity seen at the sides of the particle beginning at 4 h (Figure 2) is due to the labeling of targets bound to the side faces of the particle's probe region. RCAs were also performed in the absence of miR-210 target for the extension times seen in Figure 2 to generate appropriate control measurements for each time point. Signal arising from these particles was subtracted from the 5 amol spike signals to generate background-subtracted measurements. Although background fluorescence levels increased slightly over time, the low spot count on the 16 h control

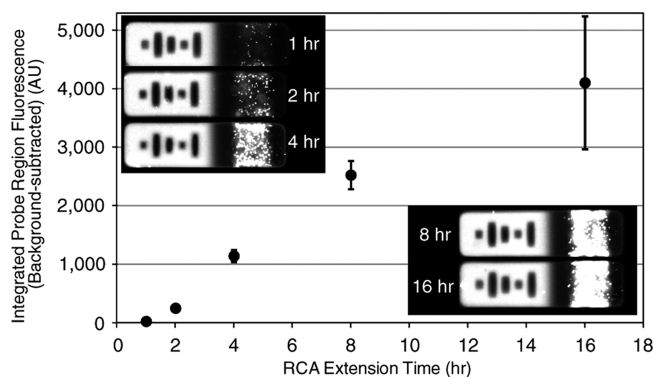


Figure 2. Background-subtracted target signal as a function of RCA extension time for 5 amol spike of synthetic miR-210. Five distinct groups of particles were exposed to the target and five distinct groups of particles were incubated without the target to obtain appropriate background measurements. For each time point, one batch with the target and one batch without the target were processed with the specified RCA extension time and then labeled using the methods detailed in the Experimental Section. Fluorescence was integrated over the probe region, with each data point representing the mean of at least five top and five bottom faces. Error bars represent the standard deviation of the signal.

particles and the absence of nonspecific binding of debris suggests that overnight extension for intense amplification is feasible for the gel-particle system. To shorten assay time, ensure that all target-binding events were detectable, and minimize signal variability, we chose to extend for 4 h for all subsequent RCA trials in this study.

Detection Performance. The optimized protocol was used to investigate the detection of miR-210 over a concentration range of 3 orders of magnitude. To simulate biological complexity and assess the specificity of the scheme, 100 ng of *E. coli* total RNA was added to each 50 μL incubation volume. As illustrated in Figure 3A, the number of spots decreased as the target amount was reduced and the code and other nonprobe-bearing portions of the gel particles exhibited very low levels of background. The low spot count on the control (0 amol) particles demonstrated that only the intended target was being captured and labeled even in the presence of a great excess of nontarget RNA sequences. It should be noted that 100 ng of total RNA is sufficient for robust multiplexed profiling with the nonamplified gel-particle protocol,¹¹ and thus profiling in total RNA with the RCA scheme would use far less input RNA (0.1–10 ng, depending on target set).¹⁰ Figure 3B shows stationary scans of particles exposed to either 0 or 5 amol of miR-210, along with a magnified fluorescence image of the probe region and the coils of reporting DNA that have formed on its top face. To assess the scheme's suitability for efficient multiplexing of low-abundance miRNA targets, we next created a batch of multi-probe particles with spatially segregated capture sequences for miR-141, miR-210, and miR-221, a panel of human miRNAs known to be frequently dysregulated in cancer profiling studies (see the Supporting Information for a movie of particle synthesis).^{1,2,11} When the three targets were added in different amounts to an incubation mix containing the multi-probe particles, the expected signal pattern was obtained upon particle analysis (Figure 3C).

To more fully characterize multiplexing performance, we developed an assay with three separate particle types designed for the detection of the three aforementioned human sequences

as well as a fourth particle type for the detection of a *C. elegans* miRNA (cel-miR-39) commonly used as an external control for quantifying RNA recovery in detection protocols that require nucleic acid extraction.^{14,15} Synthetic human miRNA targets in amounts ranging from 50 zmol to 35 amol were spiked into 50 μ L incubation volumes containing \sim 20 particles of each type and 100 ng of *E. coli* total RNA. With the exception of the 35 amol spike, the three human miRNAs were introduced simultaneously; separate spikes were performed at 35 amol to verify that target capture was probe-specific. Integrating signal intensity on the faces of the probe region provided a linear calibration curve for target amounts of 100 zmol or greater (Figure 4A). Meanwhile, counting the number of amplification spots was an effective means of calibrating the detection for all subattomole amounts investigated (Figure 4B–D). Importantly, particles bearing the probe for cel-miR-39 exhibited consistently low spot counts for all calibration trials (Figure 4A,E), indicating a high level of specificity of target capture and signal amplification.

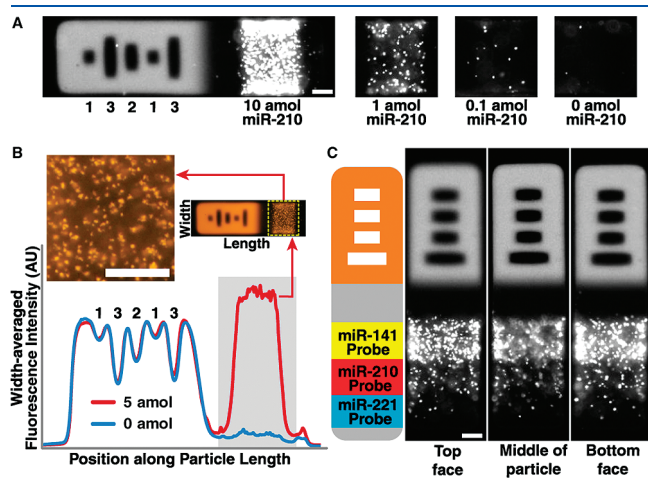


Figure 3. (A) Fluorescence images of binding events on top face of particle for detection of 10, 1, and 0.1 amol of synthetic miR-210 in buffer spiked with 100 ng of *E. coli* total RNA. (B) Overlayed stationary scans of particles exposed to solution containing either 0 or 5 amol of miR-210, with a magnified color image of the probe region. Each scan represents the mean of five top and five bottom faces. (C) Multi-probe particle exposed to solution containing 5 amol of miR-141, 1 amol of miR-210, and 0.2 amol of miR-221. The scale bars are 20 μ m.

We observed high reproducibility in detection performance at the low target levels investigated in this study. The gel particles were fabricated, encoded, and functionalized with a probe in a single step using a high-fidelity microfluidic synthesis process that provides a greater degree of reproducibility and uniformity than the multistep batch synthesis processes used to create and functionalize similar particle systems. The mean intra-trial coefficient of variation (CV) of target signal for subattomole detection with spot-counting was 14% when measuring five gel particles of each type in a given trial. By comparison, the mean intra-trial CV for attomole detection with the nonamplified scheme was 62%,¹¹ while competing particle systems require the analysis of thousands of particles for high-confidence estimates of target levels 5 000-fold higher.³⁷ With RCA on the gel particles, an inter-trial CV of 15% was calculated for three separate detections of 500 zmol of miR-210 on three separate days. LODs for each of the human miRNAs were calculated from the calibration curves in Figure 4B–D (see the Supporting Information). The lowest LOD was that of miR-141, which was detectable down to 15 zmol (\sim 9 000 copies or 300 aM in a 50 μ L incubation volume). This level of sensitivity is superior to those demonstrated by existing particle arrays, blots, RCA schemes (dumbbell, padlock blotting, branched), and conventional microarrays, and it should be sufficient for the direct profiling of highly expressed miRNAs from single cells.¹⁰ The unique hydrogel composition of our particles provides a hydrated, nonfouling scaffold that minimizes background signal from nonspecific interactions and enhances nucleic acid hybridization relative to solid surfaces. As discussed elsewhere,^{23,38–40} the three-dimensional immobilization of probe within a gel provides solution-like hybridization thermodynamics that lead to lower probe-target dissociation constants (and thus higher sensitivity) than can be obtained with solid particle systems and microarrays. Furthermore, the ability to immobilize the probe within the gel microparticles concentrates the captured targets and resulting fluorescence signal within a relatively small volume for image analysis, leading to higher sensitivity than existing RCA approaches that use well-based spectrometer measurements and Northern blots for quantification.

Serum Assay. We sought to leverage the high sensitivity and specificity of the gel-particle RCA scheme for the detection of low-abundance miRNAs in complex biological media. Recent studies have identified miRNAs as valuable blood-based biomarkers that could potentially be used for rapid, noninvasive

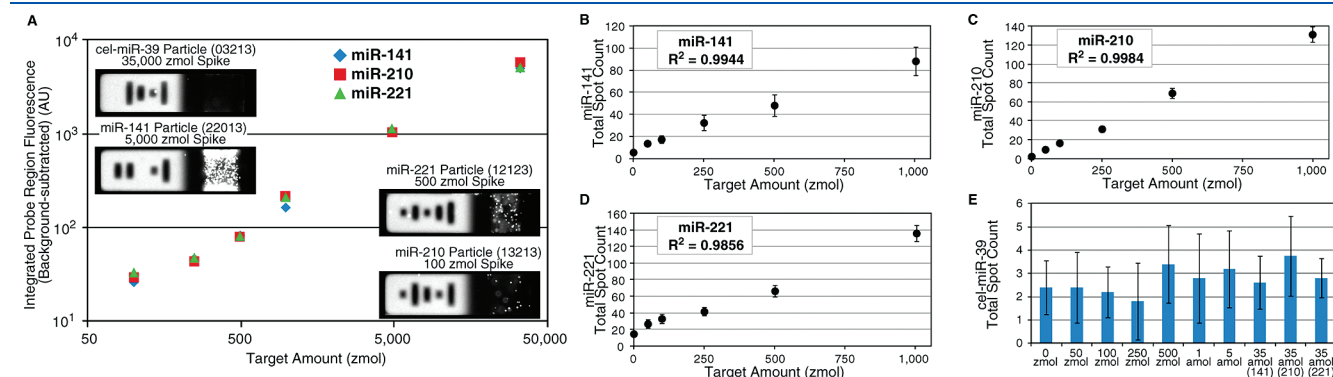


Figure 4. (A) Calibration curve for multiplexed assay. Fluorescence was integrated over the probe region for target spikes of 100–35 000 zmol. Particles bearing the probe for cel-miR-39 were used as a negative control. (B–D) Fluorescent spot counts for target spikes of 0, 50, 100, 250, 500, and 1000 zmol in a multiplexed assay. The measurement resolution demonstrated here is suitable for dysregulation profiling of targets in the subattomole range. (E) Fluorescent spot counts on cel-miR-39 particles for the calibration trials. In all trials depicted in Figure 4, 100 ng of *E. coli* total RNA was added to the incubation buffer to simulate complexity and demonstrate the specificity of the assay. Error bars represent the intra-trial standard deviation.

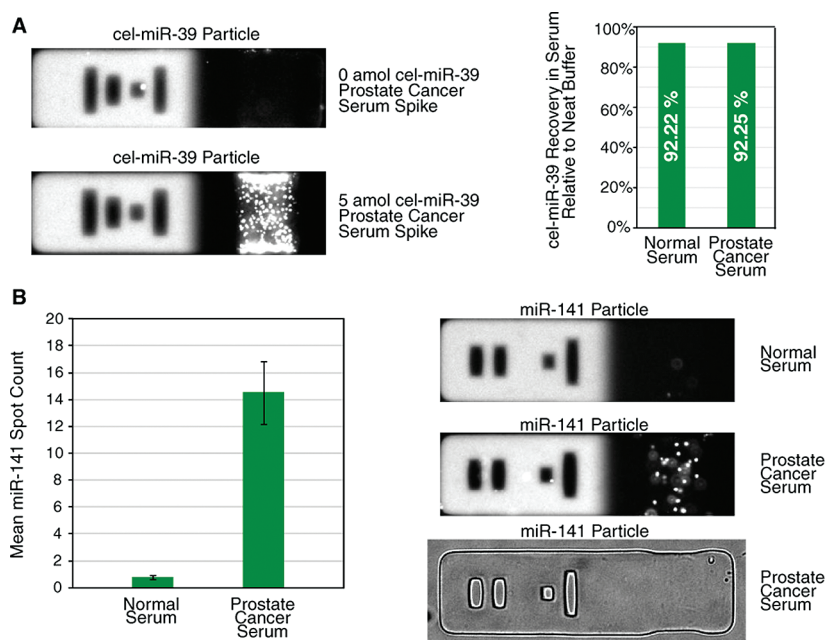


Figure 5. (A) Synthetic cel-miR-39 recovery efficiency for 5 amol spikes into normal and cancer-associated serum. (B) Upregulation of miR-141 was observed in prostate-cancer-associated serum. Data reflect the mean spot counts for three replicate trials. Error bars represent the inter-trial standard deviations.

determination of disease diagnosis and prognosis.^{14,17,18} Unfortunately, the low target abundance and complexity of blood have hindered progress in developing accurate and efficient plasma- and serum-based assays, requiring target-amplification steps and time-consuming RNA extraction protocols that complicate quantification and introduce technical variability.¹⁷ In an attempt to detect miRNA directly in 25 μ L aliquots of human serum, we modified our assay protocol by adding SDS and RNase inhibitor (SUPERase-In) to an incubation buffer that would be combined with the serum. By measurement of the recovery efficiency of synthetic cel-miR-39 spikes under a variety of conditions, it was determined that the optimal reaction mix should contain 2% SDS and 0.5 U/ μ L SUPERase-In to ensure the denaturation of both background and RISC-associated proteins as well as the inhibition of serum-based RNases.^{14,15} We spiked 5 amol of cel-miR-39 into 50 μ L mixes containing 25 μ L of either normal or prostate-cancer-associated serum and observed recovery efficiencies comparable to those measured for spikes into our previous neat incubation buffers (Figure 5A). Importantly, there was little evidence of nonspecific binding on the surfaces of the bioinert, fouling-resistant PEG-based gel particles.

We also investigated the endogenous miR-141 levels in the two serum types, seeking to confirm a previous PCR-based study that found miR-141 to be upregulated in the serum of prostate cancer patients.¹⁴ The results obtained with our gel particles for three technical replicate measurements of each serum type revealed a similar dysregulation, with mean spot counts of 0.78 ± 0.13 on particles exposed to normal serum and 14.53 ± 2.34 on those exposed to cancer-associated serum (Figure 5B). The observed copy numbers of miR-141 (<400 copies/ μ L normal, 2000 copies/ μ L cancer) also agreed with the ranges determined for the two serum types in the earlier study.¹⁴ Unlike existing detection methods, our assay required neither RNA extraction nor target-amplification steps, leading to simple and direct quantification of targets in serum without the need for data

normalization using external control measurements or primer optimization.¹⁷ Furthermore, our method required only 25 μ L of unprocessed serum for each assay. By comparison, microarray techniques that profile without target-amplification typically use 1 mL of serum to generate enough RNA extract for the assay.¹⁶

CONCLUSIONS

We have demonstrated the RCA of a universal adapter sequence selectively ligated to targets captured on encoded gel microparticles for the ultrasensitive, multiplexed profiling of miRNA. We have developed an optimized protocol that allows for the highly specific detection of subfemtomolar miRNA target concentrations in complex media, thereby expanding the dynamic range of the particle platform to over 6 orders of magnitude (300 aM to 40 pM) and introducing the possibility of direct single-cell profiling.^{10,11} Our ability to assay directly in minute amounts of readily accessible biological media could potentially be leveraged for the creation of rapid, noninvasive diagnostic tests for the profiling of focused panels of miRNAs. The incorporation of fluorescent nucleotides for reporting binding events could streamline future iterations of the assay and simplify workflow,⁴¹ while the implementation of branched RCA could be explored for digital quantification.^{42–45} It should also be straightforward to adapt the RCA scheme to a recent protein sandwich protocol developed for cytokine quantification on gel particles,²⁹ enabling the quantification of low-abundance miRNA and proteins in the same assay and perhaps even on the same particle.

ASSOCIATED CONTENT

S Supporting Information. Additional information as noted in the text. This material is available free of charge via the Internet at <http://pubs.acs.org>.

AUTHOR INFORMATION

Corresponding Author

*E-mail: pdoyle@mit.edu.

ACKNOWLEDGMENT

This work was supported by NIH Grant R21EB008814 and the Ragon Institute of MGH, MIT, and Harvard. We also acknowledge Daniel Pregibon, Rathi Srinivas, and Vincent Auyeung for helpful discussions.

REFERENCES

- (1) Lu, J.; Getz, G.; Miska, E. A.; Alvarez-Saavedra, E.; Lamb, J.; Peck, D.; Sweet-Cordero, A.; Ebert, B. L.; Mak, R. H.; Ferrando, A. A. *Nature* **2005**, *435*, 834–838.
- (2) Jiang, Q.; Wang, Y.; Hao, Y.; Juan, L.; Teng, M.; Zhang, X.; Li, M.; Wang, G.; Liu, Y. *Nucleic Acids Res.* **2008**, *37*, D98–D104.
- (3) Esquela-Kerscher, A.; Slack, F. J. *Nat. Rev. Cancer* **2006**, *6*, 259–269.
- (4) Volinia, S.; Calin, G. A.; Liu, C. G.; Ambs, S.; Cimmino, A.; Petrocca, F.; Visone, R.; Iorio, M.; Roldo, C.; Ferracin, M.; Prueitt, R. L.; Yanaihara, N.; Lanza, G.; Scarpa, A.; Vecchione, A.; Negrini, M.; Harris, C. C.; Croce, C. M. *Proc. Natl. Acad. Sci. U.S.A.* **2006**, *103*, 2257–2261.
- (5) Baker, M. *Nat. Methods* **2010**, *7*, 687–692.
- (6) Wang, H.; Ach, R. A.; Curry, B. *RNA* **2007**, *13*, 151–159.
- (7) Husale, S.; Persson, H. H. J.; Sahin, O. *Nature* **2009**, *462*, 1075–1078.
- (8) Creighton, C. J.; Reid, J. G.; Gunaratne, P. H. *Briefings Bioinf.* **2009**, *10*, 490–497.
- (9) Chen, C.; Ridzon, D. A.; Broomer, A. J.; Zhou, Z.; Lee, D. H.; Nguyen, J. T.; Barbisin, M.; Xu, N. L.; Mahuvakar, V. R.; Andersen, M. R.; Lao, K. Q.; Livak, K. J.; Guegler, K. J. *Nucleic Acids Res.* **2005**, *33*, e179.
- (10) Zhou, Y.; Huang, Q.; Gao, J.; Lu, J.; Shen, X.; Fan, C. *Nucleic Acids Res.* **2010**, *38*, e156.
- (11) Chapin, S. C.; Appleyard, D. C.; Pregibon, D. C.; Doyle, P. S. *Angew. Chem., Int. Ed.* **2011**, *50*, 2289–2293.
- (12) Birtwell, S.; Morgan, H. *Integr. Biol.* **2009**, *1*, 345–362.
- (13) Chen, J.; Lozrach, J.; Garcia, E. W.; Barnes, B.; Luo, S.; Mikoulitch, I.; Zhou, L.; Schroth, G.; Fan, J. B. *Nucleic Acids Res.* **2008**, *36*, e87.
- (14) Mitchell, P. S.; Parkin, R. K.; Kroh, E. M.; Fritz, B. R.; Wyman, S. K.; Pogosova-Agadjanian, E. L.; Peterson, A.; Noteboom, J.; O'Brian, K. C.; Allen, A.; Lin, D. W.; Urban, N.; Drescher, C. W.; Knudsen, B. S.; Stirewalt, D. L.; Gentleman, R.; Vessella, R. L.; Nelson, P. S.; Martin, D. B.; Tewari, M. *Proc. Natl. Acad. Sci. U.S.A.* **2008**, *105*, 10513–10518.
- (15) Arroyo, J. D.; Chevillet, J. R.; Kroh, E. M.; Ruf, I. K.; Pritchard, C. C.; Gibson, D. F.; Mitchell, P. S.; Bennett, C. F.; Pogosova-Agadjanian, E. L.; Stirewalt, D. L.; Tait, J. F.; Tewari, M. *Proc. Natl. Acad. Sci. U.S.A.* **2011**, *108*, 5003–5008.
- (16) Lodes, M. J.; Caraballo, M.; Suci, D.; Munro, S.; Kumar, A.; Anderson, B. *PLoS ONE* **2009**, *4*, e6229.
- (17) Brase, J. C.; Wuttig, D.; Kuner, R.; Sultmann, H. *Mol. Cancer* **2010**, *9*, 306–314.
- (18) Asaga, S.; Kuo, C.; Nguyen, T.; Terpenning, M.; Giuliano, A. E.; Hoon, D. S. B. *Clin. Chem. (Washington, DC, U.S.)* **2011**, *57*, 84–91.
- (19) Fang, S.; Lee, H. J.; Wark, A. W.; Corn, R. M. *J. Am. Chem. Soc.* **2006**, *128*, 14044–14046.
- (20) Jonstrup, S. P.; Koch, J.; Kjems, J. *RNA* **2006**, *12*, 1747–1752.
- (21) Li, N.; Jablonowski, C.; Jin, H.; Zhong, W. *Anal. Chem.* **2009**, *81*, 4906–4913.
- (22) Yao, B.; Li, J.; Huang, H.; Sun, C.; Wang, Z.; Fan, Y.; Chang, Q.; Li, S.; Xi, J. *RNA* **2009**, *15*, 1787–1794.
- (23) Pregibon, D. C.; Doyle, P. S. *Anal. Chem.* **2009**, *81*, 4873–4881.
- (24) Dendukuri, D.; Gu, S. S.; Pregibon, D. C.; Hatton, T. A.; Doyle, P. S. *Lab Chip* **2007**, *7*, 818–828.
- (25) Pregibon, D. C.; Toner, M.; Doyle, P. S. *Science* **2007**, *315*, 1393–1396.
- (26) Shingara, J.; Keiger, K.; Shelton, J.; Laosinchai-Wolf, W.; Powers, P.; Conrad, R.; Brown, D.; Labourier, E. *RNA* **2005**, *11*, 1461–1470.
- (27) Brazas, R. M.; Enos, J. M.; Duzeski, J. L.; Schifreen, R. S.; Watt, M. V. *J. Mol. Diagn.* **2006**, *8*, 671.
- (28) Blanco, L.; Bernad, A.; Lázaro, J. M.; Martín, G.; Garmendia, C.; Salas, M. *J. Biol. Chem.* **1989**, *264*, 8935–8940.
- (29) Appleyard, D. C.; Chapin, S. C.; Doyle, P. S. *Anal. Chem.* **2011**, *83*, 193–199.
- (30) Schopf, E.; Chen, Y. *Anal. Biochem.* **2010**, *397*, 115–117.
- (31) Kohro-Kawata, J.; Wener, M. H.; Mannik, M. *J. Rheumatol.* **2002**, *29*, 84–89.
- (32) Fire, A.; Xu, S. *Proc. Natl. Acad. Sci. U.S.A.* **1995**, *92*, 4641–4645.
- (33) Liu, D.; Daubendiek, S. L.; Zillman, M. A.; Ryan, K.; Kool, E. T. *J. Am. Chem. Soc.* **1996**, *118*, 1587–1594.
- (34) Zhao, W.; Ali, M. M.; Brook, M. A.; Li, Y. *Angew. Chem., Int. Ed.* **2008**, *47*, 6330–6337.
- (35) Nallur, G.; Luo, C.; Fang, L.; Cooley, S.; Dave, V.; Lambert, J.; Kukanskis, K.; Kingsmore, S.; Lasken, R.; Schweitzer, B. *Nucleic Acids Res.* **2001**, *29*, e118.
- (36) Kashkin, K. N.; Strizhkov, B. N.; Gryadunov, D. A.; Surzhikov, S. A.; Grechishnikova, I. V.; Kreindlin, E. Y.; Chupeeva, V. V.; Evseev, K. B.; Turygin, A. Y.; Mirzabekov, A. D. *Mol. Biol. (Moscow, Russ. Fed., Engl. Ed.)* **2005**, *39*, 30–39.
- (37) Peck, D.; Crawford, E. D.; Ross, K. N.; Stegmaier, K.; Golub, T. R.; Lamb, J. *Genome Biol.* **2006**, *7*, R61.
- (38) Levicky, R.; Horgan, A. *Trends Biotechnol.* **2005**, *23*, 143–149.
- (39) Fotin, A. V.; Drobyshchev, A. L.; Proudnikov, D. Y.; Perov, A. N.; Mirzabekov, A. D. *Nucleic Acids Res.* **1998**, *26*, 1515–1521.
- (40) Sorokin, N. V.; Chechetkin, V. R.; Pan'kov, S. V.; Somova, O. G.; Livshits, M. A.; Donnikov, M. Y.; Turygin, A. Y.; Barsky, V. E.; Zasedatelev, A. S. *J. Biomol. Struct. Dyn.* **2006**, *24*, 57–66.
- (41) Yan, J.; Song, S.; Li, B.; Zhang, Q.; Huang, Q.; Zhang, H.; Fan, C. *Small* **2010**, *6*, 2520–2525.
- (42) Lizardi, P. M.; Huang, X.; Zhu, Z.; Bray-Ward, P.; Thomas, D. C.; Ward, D. C. *Nat. Genet.* **1998**, *19*, 225–232.
- (43) Jarvius, J.; Melin, J.; Goransson, J.; Stenberg, J.; Fredriksson, S.; Gonzalez-Rey, C.; Bertilsson, S.; Nilsson, M. *Nat. Methods* **2006**, *3*, 725–727.
- (44) Rissin, D. M.; Kan, C. W.; Campbell, T. G.; Howes, S. C.; Fournier, D. R.; Song, L.; Piech, T.; Patel, P. P.; Chang, L.; Rivnak, A. J.; Ferrell, E. P.; Randall, J. D.; Provuncher, G. K.; Walt, D. R.; Duffy, D. C. *Nat. Biotechnol.* **2010**, *28*, 595–599.
- (45) Rissin, D. M.; Fournier, D. R.; Piech, T.; Kan, C. W.; Campbell, T. G.; Song, L.; Chang, L.; Rivnak, A. J.; Patel, P. P.; Provuncher, G. K.; Ferrell, E. P.; Howes, S. C.; Pink, B. A.; Minnehan, K. A.; Wilson, D. H.; Duffy, D. C. *Anal. Chem.* **2011**, *83*, 2279–2285.